Guide to the Impact Counters of the CDA

Emil Khalisi, Ralf Srama, Eberhard Grün

Version 1.2

Last update: 6th February 2013

Abstract

We present the impact rates of dust particles onto the Cosmic Dust Analyzer (CDA) aboard the Cassini probe. The manual introduces the “dust counters”, that evaluate the quality of an impact, as well as the access of the data, and the derivation of the most probable true density of dust.

The raw data is pre-selected and refined to a new structure that serves to a better investigation of densities, flows, and properties of interplantary dust grains. Our data is corrected for the dead time and the mis-alignments relative to the assumed Kepler orbits (pointing). The data availability ranges from DOY 150/2005 to 365/2009. The revised data is published on the website for the Magnetosphere and Plasma Science (MAPS), where it can be correlated with other *Cassini*-instruments.

Table of Contents

1 Introduction: The Cosmic Dust Analyzer 5
2 Detector Signals 6
2.1 The Entrance Grid 6
2.2 The Impact Ionisation Detector 6
2.3 The Chemical Analyser Target 7
2.4 Triggering of a measurement 7
3 Description of the Impact Counters 9
4 How to Use the Database 12
4.1 Access to the Counter Viewer 12
4.2 Data Structure `*state` 13
4.3 Output of the Data for MAPSview 14
5 Corrections to the Raw Data 17
5.1 Dead Time Correction 17
5.2 Articlulation Angle 18
5.3 Dust RAM and Sensitive Area 19
6 Adjustment of Time Scales 20

1 Introduction: The Cosmic Dust Analyzer

The Cosmic Dust Analyzer (CDA) aboard the *Cassini* spacecraft is an instrument to study the physical and chemical properties of dust particles in the interplanetary space. It consists of two subsystems working separately:

- The main sensor is the Dust Analyzer (DA) designed to analyse the particles according to their speed, mass, charge, chemistry, and pitch angle. It deploys a time-of-flight mass spectrometer. The sensitive area of the Impact Ionisation Detector (IID) is 0.0825 m^2, and Chemical Analyzer Target (CAT) is 0.0073 m^2 (Fig. 1).

- The second system is the High-Rate Detector (HRD) only counting the number of impacts with a frequency of up to 10,000 counts per second. It is a simple impact trigger with an area of 60 cm^2 (see frontpage).

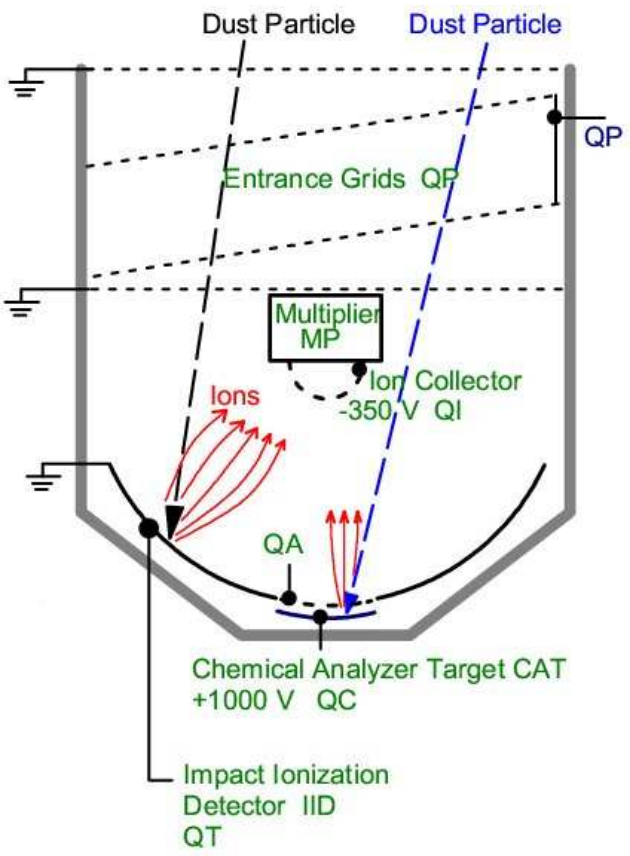

Figure 1: Schematic view of the CDA.

The DA is a sophistically working device sensitive to a broad mass range of particles: $5{\cdot}10^{-18}$ kg to 10^{-12} kg for velocities about 20 km/s. This is equivalent to a particle size of 0.1–10 micrometer. The particle detection is basically measured by four signals: QP, QT or (QC + QM), and QI (see next section, Ch. 2). They allow a rather detailed examination of the dust particle hitting the DA. — The HRD subsystem is a separately working device with its own processor and data memory. It is located at the outside of the impact bowl and detects particles with a mass larger than $8 \cdot 10^{-13}$ kg.

The general purpose is to quantify the dust density in the interplanetary space during the spacecraft cruise as well as the dust environment at Saturn. A permanent mapping of all directions is not possible because of the fixed position of the CDA on a 3-axis stabilised spacecraft. However, a designated turntable of the CDA allows some re-directioning of the boresight.

This manual introduces the so-called “dust counters” that serve to investigate local densities, particle flows, and their properties measured along the *Cassini* trajectory. The data is stored in a MySQL database on a machine at the Max-Planck-Institute for Nuclear Physics in Heidelberg, Germany. To access the data, we wrote an IDL code that returns useful graphics or correlates various physical parameters about the distribution of dust. That processed data can be found in the MAPSview database (Magnetosphere and Plasma Science) at

`http://mapsview.engin.umich.edu/ .`

Here, we explain how to access the raw data and our procedure to derive the density values from the counter rates.

2 Detector Signals

2.1 The Entrance Grid

The entrance of the DA consists of a 4-fold electric conductive grid. The two inner grids are connected to a charge amplifier such that a current (QP, "charge primary") will be induced whenever a charged particle passes by. The tilting of these two grids causes an asymmetry in the rising and declining flanks of the QP-signal and permits a precise determination of the inflow angle relative to the boresight (the boresight is the symmetry axis of the bowl). The rise time of the QP signal is proportional to the particle velocity v, and the amplitude is proportional to the charge q.

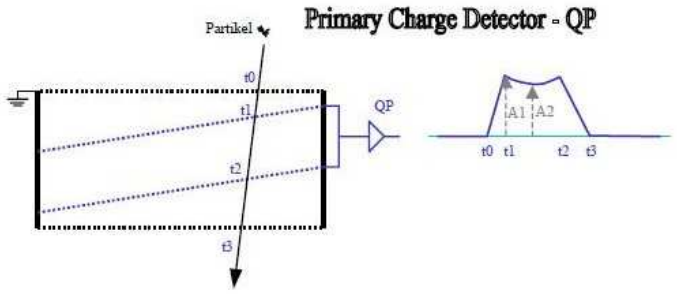

Figure 2: A charged particle induces a current at the entrance grid.

The particle mass m is estimated on the basis of some assumptions: In space, a particle carries a charge q originating from the pervasive solarwind plasma:

$$q = \sigma A \tag{1}$$

with σ being the surface charge density, and A the surface area of the particle. The dust particle is assumed as a sphere with radius $R = \frac{1}{2}\sqrt{A/\pi}$, and consists of water ice of density ρ. Then, the mass is calculated from

$$m = \rho V = \rho \cdot \frac{4}{3}\pi R^3 \tag{2}$$

$$= \frac{\rho}{6\sqrt{\pi}} \left(\frac{q}{\sigma}\right)^{\frac{3}{2}}. \tag{3}$$

q is quantified from the QP amplitude; and σ depends on the material, such that the electrostatic conditions have to be determined empirically from laboratory experiments with ice grains. An interplanetary space particle is typically charged to a surface potential of $\sigma \approx 5$ V.

The transmission at the four grids ranges between 80% and 95%, depending on the incoming angle of the dust particle. The more the angle is slanted, the lower the transmission factor. In the ideal case, the QP-signal exists for every particle registered by the the CDA.

2.2 The Impact Ionisation Detector

The inner surface of the DA is the Impact Ionisation Detector (IID). When a dust particle hits the sensitive area, it will be destroyed, eventually forming a plasma could. The positive ions are attracted by a small electric grid (-350 V, QI) that serves for focussing of the ionic fragments on a fast-responsing multiplier (QM); the electrons fall back to the surface. The transmission of the electric grid QI is 90%.

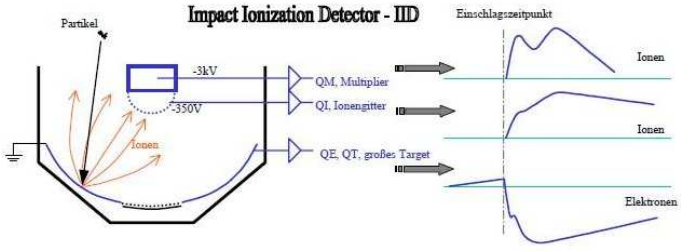

Figure 3: The ejecta of a smashed dust grain produce the currents QT on the detector wall and QI at the ion grid.

As a result, three signals are produced: QI at the ion grid and QM at the multiplier (both positive), and QT ("charge target") at the

IID (negative). The QI and QT signals are deployed to further analysis of the impact characteristics, e.g. the mass of the original particle. This determination of the particle mass m is independend from eq. 3 and goes back to the generation of charged fragments after the impact. Krüger (2003 [7]) gives the formula

$$q \sim m^{\alpha} v^{\beta}, \tag{4}$$

where q, m, and v are the ion charge, the particle mass, and the impact velocity, respectively. The values $\alpha \approx 1$ and $v \approx 3.5$, were revealed by measurements with similar dectectors aboard the *Galileo* and *Ulysses* spacecrafts (Göller & Grün, 1989 [1]). The QM signal is not utilized because it is a non-integrative channel (fast decline of the current within 10 ns), i.e. it measures only momentary currents but no particle charges. The impacts on the IID are intended to measure just the speed and the size of the grains in space.

2.3 The Chemical Analyser Target

The Chemical Analyser Target (CAT) operates in combination with the multiplier, QM, as a time-of-flight mass spectrometer. It analyses the chemical compounds of the dust particle.

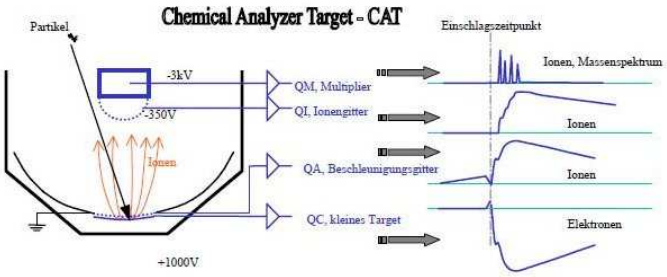

Figure 4: The QM signal provides a fast changing current that is based on the arrival times of chemical compounds of different mass.

The target itself is a segment of a sphere (radius: 8 cm) made of rhodium. It is connected to a voltage of +1000 V against the IID. A dust particle striking the CAT will be smashed and evaporised to a plasma cloud of atoms and electrons. The positively charged ions are accelerated to the electric grid QI. They will arrive sequentially in accord to their mass: hydrogen needs about 550 ns for the distance from the CAT to the electric grid, and rhodium about 5000 ns. These time-dependent arrivals of the nuclei create a current at QM that acts like a spectrometer for atomic masses. The spectoscopic lines possess information on 1) displacement of lines ($\rightarrow$ atomic number); 2) amplitudes ($\rightarrow$ abundance); and 3) line width ($\rightarrow$ isotopes).

2.4 Triggering of a measurement

The measurement of an impact starts with the generation of an electric signal, when the charged dust particle passes the entrance grid and induces a current QP. A comparator compares the QP-signal with a pre-defined threshold. Currents above the threshold would release a trigger, and the processing cycle begins: The software reads out the buffers of the channels QP, QC, QT, QI, and QM, the amplitude, rise time, base line and integral calculations, signal compression and signal storage. The entire process takes ≈800–1000 ms depending on the compression factor for the data and the frame settings (Srama 2009 [9]).

Then, the onboard flight software checks the properties of these signals to find a best-fitting classification. The ion signal amplitude, QI, is of major importance, for the event is assigned into one of 8 amplitude intervals of about one decade width. Then, other features are tested, e.g. the duration of the rise time, presence of other signals, or the number of spectral lines. The relation of the parameters are increasingly restricted, such that the event is additionally represented by a reliability tag (like 'certain', 'probable', and 'potential' dust impact). The decision process is rather complex and goes back to the experience with the *Galileo* and *Ulysses* spacecrafts (Grün *et al.* 1992 [2]). All the combined properties lead finally to a classification of the event to a distinct "counter" (Table 1). The number of that special counter is increased by one.

In summary, the basic signals which are evaluated from the impact of a dust particle are:

QP: charge, velocity, direction	
QT: energy, velocity	QC + QM: chemistry
QI: control signal at ion grid	

More details on the operating principles including a calibration and optimisation of the CDA can be found in Srama (2000 [8]).

3 Description of the Impact Counters

The “dust counters” are an array of 27 numerators (previously 19) for certain impact properties. Each impact is analysed by the onboard flight software immediately after its occurence. A dust grain hitting the sensitive area of the detector will produce various signals that are subject to a classification. The combined properties of the signals are interpreted by a decision making algorithm, so the counters serve as “containers” or “categories” for some common characteristics of the dust particles. These characteristics provide a qualitative nomenclature, e.g. “strong” or “weak” event without quantifying it. Their names and their features are given in Table 1. The objective is to accumulate the impacts with special features in order to compare their frequency of occurrence.

The algorithm is strongly priority-sequenced. For example, the first check is whether the necessary signals are present, otherwise the event is sorted as “noise” (#14, N1). Afterwards, the criteria for strong impacts on the CAT are checked (#0 – #3, A0 – A3). When all essential conditions are met, the counter value is enhanced by 1, and the search procedure terminates. If not, the next criteria are checked unless an appropriate counter will be found. Each impact is assigned to a unique counter.

Table 1: Description of the counters and the thresholds for the QI signal in digital numbers dn (Srama, 2000 [8]).

counter #	**name**	**QI signal**	**description**	**priority**
0	A0	$> 3.29{\cdot}10^{-12}$ C (200 dn)	CAT big, >3 mass lines	2
1	A1	$> 1.66{\cdot}10^{-12}$ C (170 dn)	CAT medium, >3 mass lines	3
2	A2	$> 6.71{\cdot}10^{-13}$ C (130 dn)	CAT big, 2 mass lines	4
3	A3	$> 3.31{\cdot}10^{-13}$ C (100 dn)	CAT medium, 2 mass lines	5
4	A4	$> 1.45{\cdot}10^{-13}$ C (70 dn)	CAT small, 2 mass lines	15
5	A5	$> 5.82{\cdot}10^{-14}$ C (45 dn)	CAT tiny, 2 mass lines	17
6	A6	$> 2.57{\cdot}10^{-14}$ C (30 dn)	CAT small, no lines	18
7	A7	$> 1.03{\cdot}10^{-14}$ C (20 dn)	CAT medium, relaxed	16
8	I0	$> 2.62{\cdot}10^{-12}$ C (190 dn)	IID very big	8
9	I1	$> 1.32{\cdot}10^{-12}$ C (160 dn)	IID big + fast	9
10	I2	$> 6.71{\cdot}10^{-13}$ C (130 dn)	IID medium + fast	10
11	I4	$> 1.45{\cdot}10^{-13}$ C (70 dn)	IID big + slow	11
12	I5	$> 5.82{\cdot}10^{-14}$ C (45 dn)	IID medium + slow	12
13	BO	strong	both targets (QC + QT)	22
14	N1	QI flare	Noise: signals on QT only	1
15	S0		spare: no function	23
16	A8	$> 9.06{\cdot}10^{-16}$ C (12 dn)	CAT tiny, 2 mass lines	20
17	I3	$> 3.31{\cdot}10^{-13}$ C (100 dn)	IID small + fast	13
18	I6	$> 1.75{\cdot}10^{-14}$ C (25 dn)	IID small + slow	14
19	I7	$> 3.04{\cdot}10^{-15}$ C (14 dn)	IID tiny	21
20	WO	$> 1.75{\cdot}10^{-14}$ C (25 dn)	Wall impact medium	6
21	W1	$> 1.95{\cdot}10^{-15}$ C (13 dn)	Wall impact tiny	7
22	N0		Noise: high baseline on QC	19
23	N2		Noise: any other signals	24
24	T0		Test pulse: o.k.	A1
25	T1		Test pulse: wrong	A2
26	E0		internal interrupt counter	–

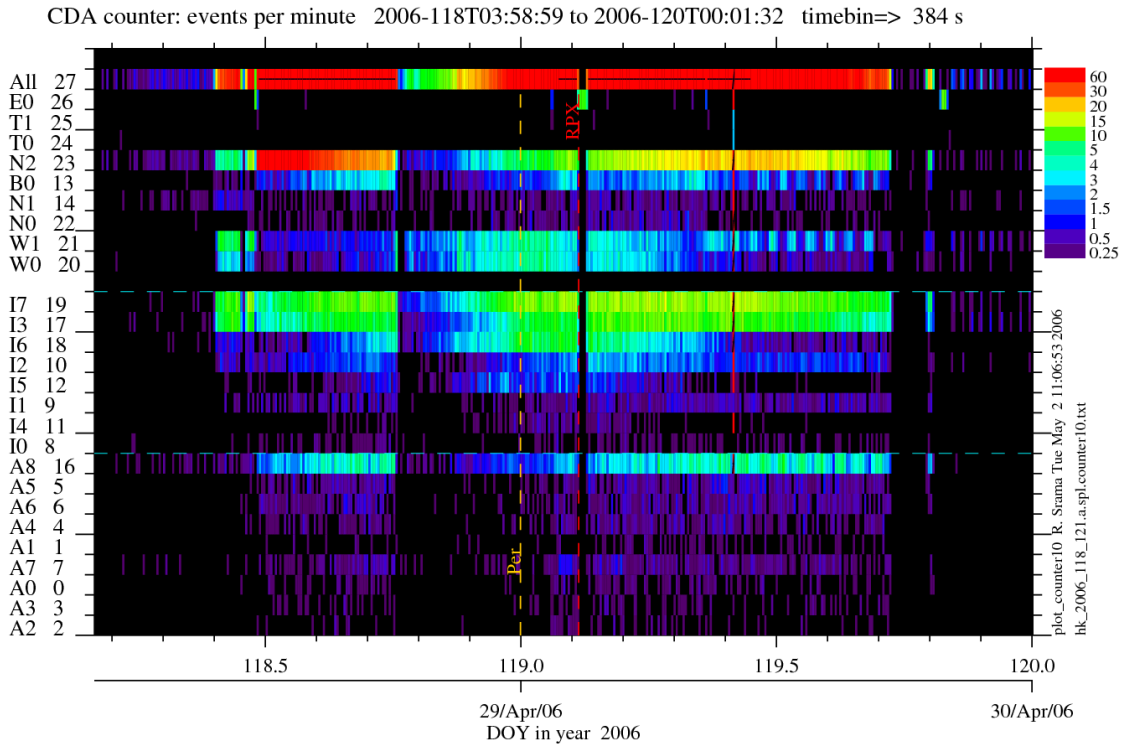

Figure 5: Counter data of DOYs 118 and 119 of 2006. The orange dashed line is the moment of perikronium, the red dashed line denotes the ring plane crossing.

The classification scheme follows a threefold pattern:

- A0 – A8: counter names for the CAT. These are signals showing mass lines on the multiplier (QM) with a corresponding QC signal; the impacts are further divided into 9 sub-classes (0 to 8) for large, medium, small responses as well as the number of the spectral lines on QM.
- I0 – I7: counter names for impacts on the IID; further division into 8 sub-classes (0 to 7) for fast and slow entrance velocities (QP signal).
- others: ten more counters are for putative noise records, impacts on the non-sensitive area ("wall"), test pulses, and control modes.

The counter values are stored in a comprehensive IDL data base. Fig. 5 shows an example for the impacts per minute on each counter (vertical axis). The lower third of the figure (blue dashed line) gives information about the CAT-impacts, the middle is for the IID-impacts, and the upper is for the non-classified events. The uppermost row summarizes the total of all counters.

In the course of the mission, the definitions experienced various changes, and so did the flight software. An overview of the software versions are given in the adjacent table. Moreover, the thresholds for the registration of a particle are altered to adjust for the ambiences of a particular orbit: dense regions, ring plane crossings, flybys at moons etc. For example, when flying through a dense cloud, the number of very small particles is high and large impacts are rarely triggered (see Ch. 5.1). Then, the "masscut" was lifted which resulted in a lower mode of sensitivity of the CDA. Therefore, the data is a *relative* measure at different environments and should be taken with care.

from DOY	to DOY	FSW version
1998-353	1999-235	7.0.0
1999-236	2002-133	7.2.0
2002-134	2002-333	8.4.0
2002-334	2003-146	9.0.0
2003-147	2002-125	9.0.2
2004-126	2004-228	9.2.0
2004-229	2005-149	9.2.4
2005-150		10.0.0

The counters were originally not meant for scientific use, but rather to roughly prioritise the events for the data readout from the repository on the spacecraft. The bandwidth is limited to 524 kps, though it cannot guarantee the download of all strong impacts of interest. Thus, the change of thresholds at the channels was to select more important dust records for a transfer than noise events which happen more often (Srama, 2009 [9]). The concept of the counters turned out to be interesting for correlations with properties that have been measured by other *Cassini* instruments. Still, we have to be aware of the biases that come along with these counters. The particle rates have to be corrected for insensitive times and misalignments of the CDA. The data we present here are corrected for all these items as described in the next sections.

4 How to Use the Database

The data returned from the spacecraft is divided into different packages like instrument status, housekeeping data, counter data, and science data. They are stored in a database which is founded on a MySQL architecture. The basics are described in the guide “CDA Database” by Kempf (2006a [3]): properties and operation of the instrument, processing of data, its products, the structure of the database, and the access. The accompanying manual “CDA Data Processing Tool” by Kempf (2006b [4]) introduces to the GUI data viewer, called “Browser”, that provides a graphical access to all datasets.

4.1 Access to the Counter Viewer

The Browser software is written in the Interactive Data Language (IDL). It incorporates various tools, one of which is the *CounterAnalyser*. To open that Browser, you need the access rights to the host machine, your user name, and your password. At present, the access is given via the host `pallene.mpi-hd.mpg.de`. Compile the routines for the browser and initiate the tool “countergui”:

```
IDL> @browser_compile
```
.... (the progress is shown)...

```
IDL> countergui
```
.... (compilation of kernels)...

The Browser window will open (Fig. 6). The database can be accessed by selecting the observational interval from the pull-down menu “Data Base” → “Load Data”. A smaller query window pops up, and the user is asked to confirm the access as well as specify the time interval of data in the two fields “Load data from... to...”. Then, press “Query DB” at the bottom of the query window, and you are in.

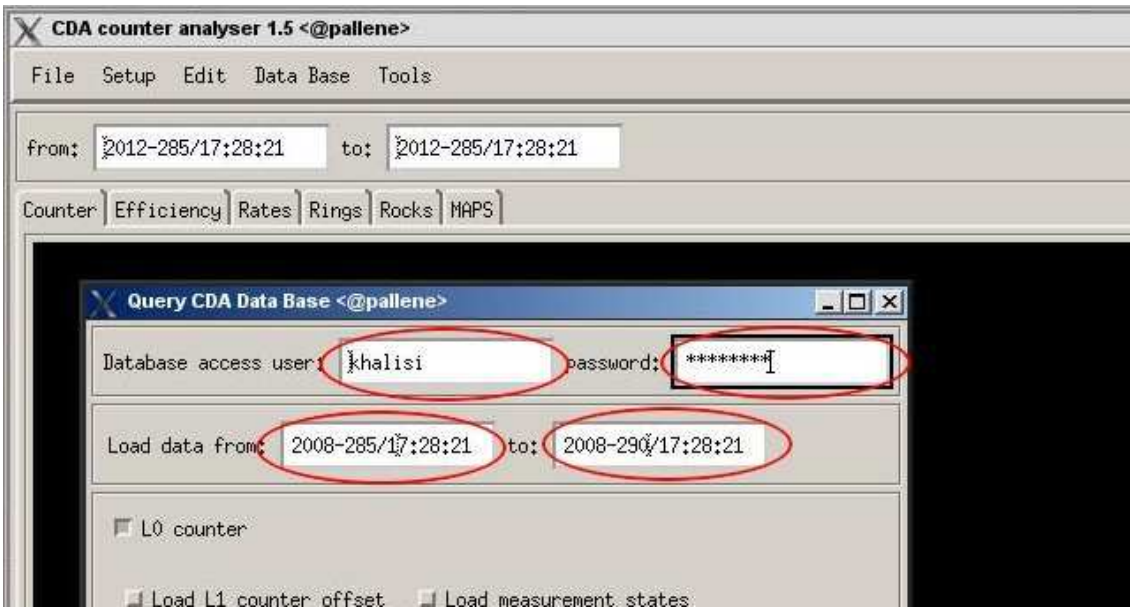

Figure 6: Menue of the CDA Browser.

The counter data of the selected time will be loaded, and the measurements are visualised in the six panels “Counter”, “Efficiency”, “Rates”, “Rings”, “Rocks”, and “MAPS”. The time interval can be further limited in the “from” and “to” field, whereupon the boundaries have to be inside the range specified in the small query window.

4.2 Data Structure `*state`

The key parameters of any impact are internally stored in an IDL-structure called `*state`. It can be accessed via the IDL command

```
IDL> HELP, *state, /struc
```

The output is shown in Table 2. This structure is a collection of scalars, arrays, or other variables which, in turn, can contain more sub-structures. They are, for example, strings specifying the time and date of a particular event, access data, or spacecraft properties, respectively. The entire structure `*state` returns a total of 96 tags. Table 2 shows the first 19 plus the last one.

The tag in eighth line of Table 2, `CNT`, is an IDL pointer that directs to another (sub-)structure named `(*state).cnt` . The latter one can be accessed by the analogue command as above when replacing `*state` by `(*state).cnt` . This output is listed in Table 3.

The sub-structure `(*state).cnt` retains itself a total of 20 tags. The first field is called `SCLK` which is an integer of type LONG and stores the spacecraft clock; the second field is the Julian Date `JD` which is of floating point type; the third is the array `COUNTER` of type LONG storing the 27 counter classes (Table 1) for the impact events as evaluated by the flight software. The other parameters are information about the pointing of the CDA; the position of the spacecraft; its distance to celestial bodies (Sun, Jupiter, Saturn, Enceladus, Titan, xxx, ring plane); etc. This data of Table 3 is what we would call the “original counter data”.

The comparison of dust particles is impaired by the ever-varying measurement constraints (see Ch. 3): The modification of the thresholds for the recording of an impact puts a bias on the properties, thus, the counter classes embody rather a qualitative evaluation than a quantitative. This means that quantities like mass and velocity are calculated relative to the environment and named “weak”, “strong”, “fast”, etc. In practice, this procedure turned out successful, for the results did not ruin the scientific investigation of the phenomenon itself. The precision may be affected, though.

Table 2: Excerpt of the IDL structure `*state`. Only the first 19 of the 96 as well as the last data fields are shown.

```
** Structure <10f7c48>, 96 tags, length=1032, data length=976, refs=1:
   VERSION         FLOAT           1.52000
   PRODUCED        DOUBLE          2455783.9
   CHANGED         DOUBLE          2455783.9
   USER            STRING    '*****'
   HOST            STRING    '*****'
   PASSWD          STRING    '*****'
   NMODES          INT             6
   CNT             POINTER   <PtrHeapVar15>
   HRD             POINTER   <NullPointer>
   DA              POINTER   <NullPointer>
   ROCK            POINTER   <NullPointer>
   RATE            POINTER   <NullPointer>
   MODEL           POINTER   <NullPointer>
   CNTOFFSETL0     LONG      Array[27]
   CNTOFFSETL1     LONG      Array[27]
   CNTOFFSETSCLK   LONG            0
   N               INT             0
   T_RANGE         DOUBLE    Array[2]
   T0              DOUBLE          2453954.5
   .....           .....     .....
   DB_USEVELRANGE  FLOAT     Array[2]
```

Table 3: Content of the IDL structure `(*state).cnt`, which is a sub-structure of `*state` of Table 2. This example displays data from day 2006-220T09:45:00.

```
** Structure <13467b8>, 20 tags, length=248, data length=236, refs=1:
   SCLK            LONG        1533721703
   JD              DOUBLE           2453955.9
   COUNTER         LONG      Array[27]
   CDA_BORES       FLOAT     Array[4]
   SC_POS          FLOAT     Array[3]
   SC_VEL          FLOAT     Array[3]
   SC_RA           FLOAT           225.000
   SC_DEC          FLOAT          -35.2644
   SC_DIST_SUN     DOUBLE       1.6735639e+09
   SC_DIST_JUP     DOUBLE          -1.0000000
   SC_DIST_SAT     DOUBLE           2783391.2
   SC_DIST_ENC     DOUBLE       1.0711034e+08
   SC_DIST_TIT     DOUBLE       1.0187969e+08
   SC_DIST_ROT     DOUBLE           2753746.6
   SC_DIST_RPC     DOUBLE          -2212217.4
   VDUST           FLOAT           2.51650
   MEASSTATE       INT              1
   VERSION         INT              2
   OFFSET          INT              0
   SRC             INT              1
```

In mid-2005, the counter definitions were revised as a consequence of a new software. The counter classes were re-arranged and their number enlarged from 19 to 27 counters. That change made a direct comparison between the "old" and "new" impact properties even more difficult. We merged the counters of similar type to a congeneric group and compiled a matrix as in Table 4. The impacts on the CAT and IIT, repectively, were subsumed, and the group of "wall" impacts was created. The test pulses and interrupt signals remain unused. The counter group "iitbig" is a subset of "iit".

Group name	Counters (before DOY 150/2005)	Counters (after DOY 150/2005)
noise	#5 + #19	B0 + N0 + N2
wall	(undefined)	W0 + W1
cat	#2 + #3 + #9 + #12 + #13 + #15 + #17	A0 + A1 + A2 + A3 + A4 + A5 + A6 + A7 + A8
iit	#6 + #7 + #10 + #11 + #14	I0 + I1 + I2 + I3 + I4 + I5 + I6 + I7
iitbig	#6 + #7	I0 + I1 + I2 + I4 + I5
qi	#16	N1
all	noise + cat + iit + qi	noise + wall + cat + iit + qi

Table 4: Counters of Table 1 are merged to six groups. See text for details.

4.3 Output of the Data for MAPSview

The Browser provides the tab "MAPS" (Fig. 6). On switching to it, the original counter data will be processed and the dust rates for the counter groups of Table 4 generated. They can be accessed via the MAPSview database for the DOYs from 150/2005 to 365/2009 as available. More comprehensive data can be obtained from the instrument PIs. The MAPSview files are named

`CDA__CNTS_`*YYYYDOY*`.TAB`, where YYYY is the specified year and DOY the day of the year. An excerpt of the data file is shown on page 16. The setup is organised as follows:

- first three colums: civil time of data readout, the Julian Date, and the time leap dT, respectively;
- fourth column: number of registered impacts dN as explained in Chapter 5, eq. (6);
- next seven colums: corrected particle rates $r'_{(\mathrm{group})}$ (see Chapter 5.1) for each of the six impact groups of Table 4 plus the combined rate for all counters;
- last three colums: sensitive area A_{eff}, the dust velocity v_{dust}, and the particle density n.

The IDL-format of the row is:
`A, X, F16.7, I5, I5, X, 7(F10.6,X), F12.8, X, F10.4, 2X, E10.4`

Date/Time	Jul.Day	dT	dN	r'_{noise}	r'_{wall}	r'_{cat}	r'_{iit}	r'_{iitbig}	r'_{qi}	r'_{all}	A_{eff}	v_{dust}	n
2006-251T04:58:35	2453986.7073531	64	42	0.000000	0.000000	0.000000	0.000000	0.000000	1.124082	1.124082	0.07187760	6190.0418	2.5265E-03
2006-251T04:59:39	2453986.7080938	64	39	0.000000	0.000000	0.000000	0.022289	0.000000	0.846973	0.869262	0.07187760	6190.0418	1.9537E-03
2006-251T05:00:43	2453986.7088345	64	40	0.000000	0.000000	0.000000	0.000000	0.000000	0.946970	0.946970	0.07187760	6192.4173	2.1276E-03
2006-251T05:01:47	2453986.7095753	64	42	0.000000	0.000000	0.000000	0.026764	0.000000	1.097319	1.124082	0.07187760	6192.4173	2.5255E-03
2006-251T05:02:51	2453986.7103160	64	45	0.000000	0.000000	0.000000	0.000000	0.000000	1.458093	1.458093	0.07187760	6194.7936	3.2747E-03
2006-251T05:03:55	2453986.7110567	64	41	0.000000	0.025162	0.000000	0.000000	0.000000	1.006481	1.031643	0.07187760	6194.7936	2.3169E-03
2006-251T05:04:59	2453986.7117975	64	40	0.000000	0.023674	0.000000	0.000000	0.000000	0.923295	0.946970	0.06967440	6197.1740	2.1932E-03
2006-251T05:06:03	2453986.7125382	64	39	0.000000	0.000000	0.000000	0.000000	0.000000	0.869262	0.869262	0.06967440	6197.1740	2.0132E-03
2006-251T05:07:07	2453986.7132789	64	45	0.000000	0.032402	0.000000	0.000000	0.000000	1.425691	1.458093	0.06967440	6199.5570	3.3756E-03
2006-251T05:08:11	2453986.7140197	64	41	0.000000	0.000000	0.000000	0.025162	0.000000	1.006481	1.031643	0.06967440	6199.5570	2.3883E-03
2006-251T05:09:15	2453986.7147604	64	43	0.000000	0.028493	0.000000	0.000000	0.000000	1.196724	1.225217	0.06967440	6201.9426	2.8354E-03
2006-251T05:10:19	2453986.7155011	64	41	0.000000	0.000000	0.000000	0.000000	0.000000	1.031643	1.031643	0.06967440	6201.9426	2.3874E-03
2006-251T05:11:23	2453986.7162419	64	43	0.000000	0.000000	0.000000	0.000000	0.000000	1.225217	1.225217	0.06967440	6204.3307	2.8343E-03
2006-251T05:12:27	2453986.7169826	64	40	0.000000	0.000000	0.000000	0.023674	0.000000	0.923295	0.946970	0.06967440	6204.3307	2.1906E-03
2006-251T05:13:31	2453986.7177234	64	42	0.000000	0.000000	0.000000	0.000000	0.000000	1.124082	1.124082	0.06967440	6206.7213	2.5993E-03
2006-251T05:14:35	2453986.7184641	64	37	0.000000	0.000000	0.000000	0.000000	0.000000	0.732054	0.732054	0.06967440	6209.1144	1.6922E-03
2006-251T05:15:39	2453986.7192048	64	45	0.000000	0.000000	0.000000	0.000000	0.000000	1.458093	1.458093	0.06967440	6209.1144	3.3704E-03
2006-251T05:16:43	2453986.7199456	64	45	0.000000	0.000000	0.000000	0.000000	0.000000	1.458093	1.458093	0.06967440	6211.5101	3.3691E-03
2006-251T05:17:47	2453986.7206863	64	40	0.000000	0.000000	0.000000	0.000000	0.000000	0.946970	0.946970	0.06967440	6211.5101	2.1881E-03
2006-251T05:18:51	2453986.7214270	64	37	0.000000	0.000000	0.000000	0.000000	0.000000	0.732054	0.732054	0.07187760	6213.9083	1.6390E-03
2006-251T05:19:55	2453986.7221678	64	44	0.000000	0.000000	0.000000	0.000000	0.000000	1.336131	1.336131	0.07187760	6213.9083	2.9915E-03
2006-251T05:20:59	2453986.7229085	64	40	0.000000	0.000000	0.000000	0.000000	0.000000	0.946970	0.946970	0.07187760	6216.3074	2.1194E-03
2006-251T05:22:03	2453986.7236492	64	43	0.000000	0.000000	0.000000	0.000000	0.000000	1.225217	1.225217	0.07187760	6216.3074	2.7421E-03
2006-251T05:23:07	2453986.7243900	64	36	0.000000	0.000000	0.000000	0.000000	0.000000	0.671419	0.671419	0.07187760	6218.7107	1.5021E-03
2006-251T05:24:11	2453986.7251307	64	40	0.000000	0.023674	0.000000	0.000000	0.000000	0.923295	0.946970	0.07187760	6218.7107	2.1186E-03
2006-251T05:25:15	2453986.7258715	64	40	0.000000	0.000000	0.000000	0.000000	0.000000	0.946970	0.946970	0.07187760	6221.1167	2.1177E-03
2006-251T05:26:19	2453986.7266122	64	39	0.000000	0.000000	0.000000	0.000000	0.000000	0.869262	0.869262	0.07187760	6221.1167	1.9440E-03
2006-251T05:27:23	2453986.7273529	64	41	0.000000	0.025162	0.000000	0.000000	0.000000	1.006481	1.031643	0.07187760	6223.5251	2.3062E-03
2006-251T05:28:27	2453986.7280937	64	42	0.000000	0.000000	0.000000	0.000000	0.000000	1.124082	1.124082	0.07187760	6223.5251	2.5129E-03
2006-251T05:29:31	2453986.7288344	64	44	0.000000	0.000000	0.000000	0.000000	0.000000	1.336131	1.336131	0.07187760	6225.9361	2.9857E-03
2006-251T05:30:35	2453986.7295751	64	40	0.000000	0.000000	0.000000	0.000000	0.000000	0.946970	0.946970	0.07187760	6228.3496	2.1153E-03
2006-251T05:31:39	2453986.7303159	64	42	0.000000	0.000000	0.000000	0.000000	0.000000	1.124082	1.124082	0.07187760	6228.3496	2.5109E-03
2006-251T05:32:43	2453986.7310566	64	37	0.000000	0.000000	0.000000	0.000000	0.000000	0.732054	0.732054	0.07187760	6230.7657	1.6346E-03
2006-251T05:33:47	2453986.7317973	64	39	0.000000	0.000000	0.000000	0.000000	0.000000	0.869262	0.869262	0.07187760	6230.7657	1.9410E-03
2006-251T05:34:51	2453986.7325381	64	33	0.000000	0.000000	0.000000	0.000000	0.000000	0.515938	0.515938	0.07187760	6233.1843	1.1516E-03
2006-251T05:35:55	2453986.7332788	64	35	0.000000	0.017584	0.000000	0.000000	0.000000	0.597870	0.615454	0.07187760	6233.1843	1.3737E-03
2006-251T05:36:59	2453986.7340195	64	36	0.000000	0.000000	0.000000	0.000000	0.000000	0.671419	0.671419	0.07187760	6235.6055	1.4980E-03

Table 5: Sample of the counter file `CDA__CNTS_2006251.TAB` that contains the particle rates and conditions of the CDA. See text for details.

5 Corrections to the Raw Data

The local particle density n is calculated by

$$n = \frac{dN}{dV} = \frac{r'}{A_{\mathrm{eff}} \cdot v_{\mathrm{dust}}}, \tag{5}$$

where dN denotes the number of particles in the space volume dV, and r' is the true counter rate, A_{eff} the sensitive area of the CDA that is exposed to the direction of the dust flow ("dust-RAM"), and v_{dust} the relative velocity of the dust particles to the spacecraft. The raw data in the `*state`-pointer does not provide any of the three quantities on the right side of eq. (5), but they can be determined after corrections from biases as discussed below.

The counters are integer values. They are read out on a semi-regular time period of $dT = t_j - t_{j-1} = 64$ seconds. Due to buffering effects and interrupts, the standard interval can be split to fractions (e.g. 35 + 29 sec or 40 + 24 sec), and multiples of 64 can occur. Such interrupts are always two-part, and never consist of three or more fragments. In some cases, the two fragments happen to be divided by one or more 64-sec-intervals which slipped between them. In that case, we added the first fragment to the previous time interval, while the second one to the subsequent interval at the end of the "unregularity". This ensures that no periods less than the standard of approximately 64 seconds occur.

The impact rate r is calculated by

$$r = \frac{dN}{dT} = \frac{N_j - N_{j-1}}{t_j - t_{j-1}}, \tag{6}$$

where N_j and N_{j-1} are the particle numbers for one specified counter group of Table 4, and dT is the corresponding period of measurement.

5.1 Dead Time Correction

The procedure of determining and storing each impact event takes up to 1 second (see Chapter 2.4). While evaluating the counter class, the Dust Analyser is insensitive to other impacts, i.e. the instrument will stay in a "dead time". The next measurement will only be possible when the recording process has finished. This finite response time causes an error in the determination of the true dust density in space: In dense regions, when the instrument is expected to go into saturation ($N_j - N_{j-1} \gtrsim 60$), the impact rate will be underestimated systematically.

Since the statistics of dust impacts is based on the Poisson process, a reconstruction of the "true" rate, r', is possible as much as the statistical distribution of the impact times is known. The details of the correction procedure are discussed by Kempf (2008 [5], 2012 [6]). To correct for the dead time of the impact rates, we deploy the formula

$$r' = 60.0 \frac{r}{1 - \tau r}, \tag{7}$$

where $\tau = 0.94$s is the mean dead time of an individual event (Srama 2009 [9], his equation 3.43). The dimension is [min^{-1}]. This formula is easy to handle and yields almost identical results for a moderate impact frequency. Only if the instrument runs into saturation with impact frequencies ≈ 0.98 s^{-1}, the error exceeds 20% with respect to the formula by Kempf (2008 [5]).

(*** Kempf-Methode als alternativen Code konstruieren und erläutern ***)

5.2 Articlulation Angle

When the *Cassini* spacecraft was designed, it incorporated a movable platform for its instruments. In 1991/92, a re-design gave rise to the abandonment of that plattform. The spacecraft had a 3-axis stabilisation, so the instruments could not cover all directions for their field of view. If special attention was needed by a device, the whole spacecraft had to be swung. Thus, all measurement campains had to be planned precisely in time with only a litte degree of freedom. The omission of the general platform became a major disadvantage for the scientific observations.

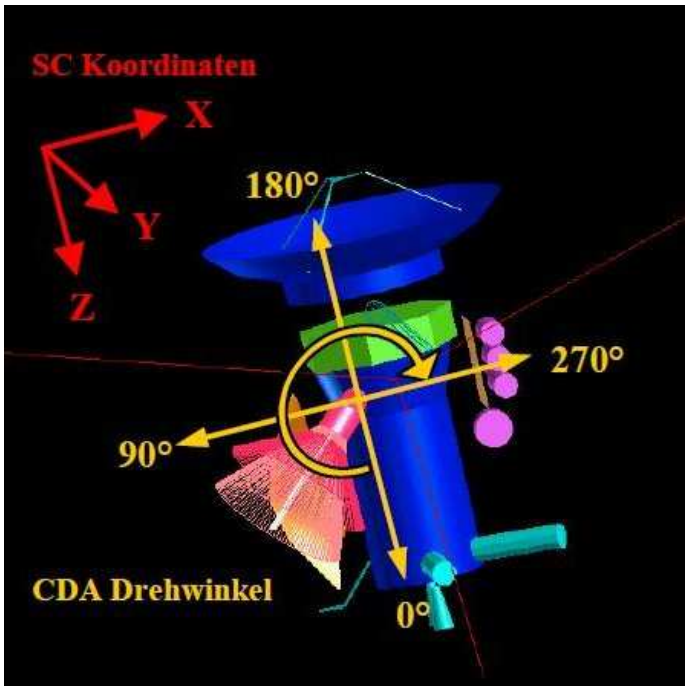

Figure 7: The articulation angles of the CDA are the revolutions of the turntable on which the device is mounted.

The CDA team decided to build an own pivoting table for the dust analyser to enable a little alignment to other lines of sight. The rotation of this turntable is called “articulation”. It can be pivoted from 0° to 270°. The zero-angle points towards the rear of the spacecraft (Fig. 7). The rotation can be performed with 8 different velocities, a typical value is 90° per 10 minutes.

Note, that the articulation angle is only a one-dimensional deviation of the aperture relative to the orientation of the spacecraft (z-axis); it comprehends neither information about the direction of dust flow nor the direction of flight of the spacecraft. The articulation angle is used to achieve some little liberty when the spacecraft is aligned unfavourably. In order to scan all directions, the spacecraft itself would have to revolve permanently. The angle “boresight” (described in the next section) is of great importance, because it reflects the alignment of the CDA relative to Saturn’s center (kronographic coordinates).

The articulation angle and its epoch of latest allocation are stored in the data base in the pointers `(*state).art_a` and `(*state).art_jd`, respectively (Table 2, not shown in the list). The values are changed on irregular time scales (typically once or twice per day). Sometimes they may stay the same for a couple of days. For our data base, the values were extracted from the two pointers without editing. In the data file they are incorporated to the sensitive area of the CDA, A_{eff}.

5.3 Dust RAM and Sensitive Area

As the spacecraft moves along her trajectory, the orientation of the aperture (pointing of the boresight) will gradually change relative to other bodies in space. The articulation enables a pivoting around an axis perpendicular to the spacecraft's z-axis (Ch. 5.2), but the orientation relative to the dust flow is still not considered.

In deed, the particles can enter the CDA from any direction, since they could be part of a stream with unknown origin, or rubble piles, or stray bullets from a physical collision, or interlopers from interstellar space etc. Because of the lack of detailed information about the planetologic conditions, one assumption has to be made a priori, which is *not* necessarily true: The particle is supposed to be on a Kepler orbit around Saturn before having hit the CDA. That Kepler orbit marks the only trajectory to be reliably calculated. The angle between the aperture axis (boresight) and the *supposed* flow of these particles is called the "dust ram" (Fig. 8).

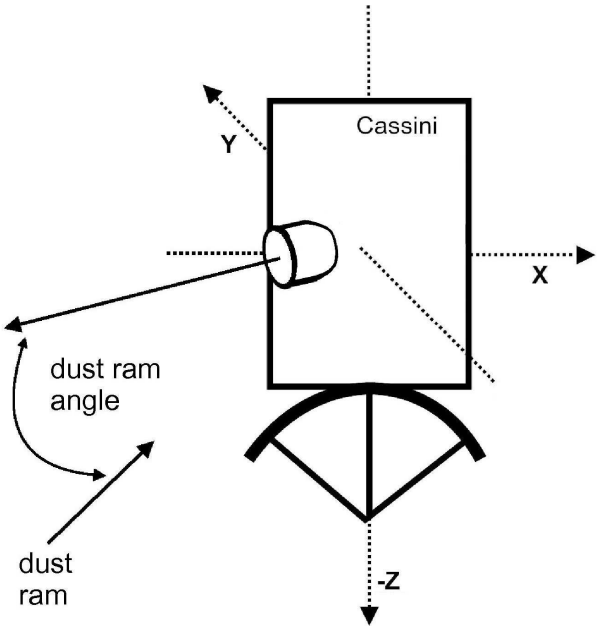

Figure 8: The pointing of the CDA may deviate from the dust ram and, thus, expose only a part of its sensitive area.

The angle of the dust ram α is taken from an auxiliary file that stores the pointings of the CDA. It is checked whether or not a Keplerian particle could be registered, for the sensitive area $A_{\rm eff}$ of the instrument being exposed to the dust ram. Figure 9 displays the projection of the sensitive area for different tilts of dust flows. If the angle α is larger than 47°, the impact is assumed to be on a non-Keplerian orbit and not contributing to the local dust density ($A_{\rm eff} = 0$). For the central segment of the CDA, as formed by the CAT, the maximum tilt off the head-on direction will be even lower, ca. 30°.

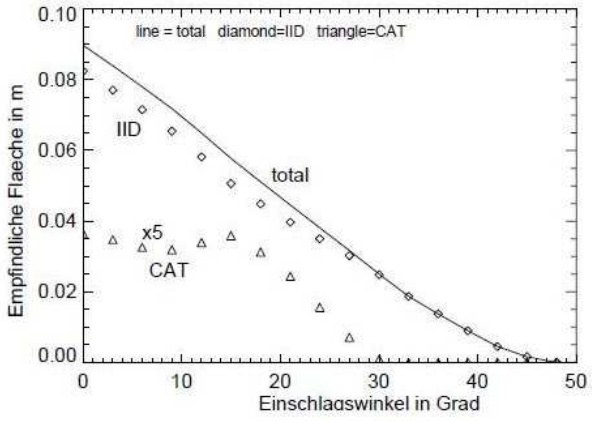

Figure 9: Effective surface area [in m^2] of the IID and CAT as a function of the entrance angle of a particle. The values for the CAT are enhanced by a factor 5 for a better visibility (Srama 2000 [8]).

The velocity $v_{\rm dust}$ of the particles can be obtained from the difference of their Keplerian velocity and the speed of the spacecraft $v_{\rm Cass}$:

$$v_{\rm dust} = v_{\rm Kepler} - v_{\rm Cass} \quad (8)$$

$$= \sqrt{\frac{GM_{\rm S}}{a}} - v_{\rm Cass}, \quad (9)$$

where G is the Gravitational constant, $M_{\rm S}$ the mass of Saturn, and a the distance of the particle from the planet's center. $v_{\rm Cass}$ is taken from the ephemeris data. The modulus $|v_{\rm dust}|$ yields the impact velocity of the dust grain independent of the QP-signal (cf. Chapter 2).

6 Adjustment of Time Scales

The ephemeris file provides the data at an interval of 120 seconds, while the counter data in the `*state`-pointer scales on a semi-regular period of 64 seconds (the latter is due to read-outs by the flight software, s. Ch. 5.1). The two different time scales are merged by the simple condition

$$t_i \leq t_{j1\ldots jn} < t_{i+1}, \tag{10}$$

where the index i runs through the rougher-meshed time scale (ephemeris data), and j are the fine-meshed tick marks (counter data). Thus, some marks of the counter data $t_{j1}...t_{jn}$ (with n being 2 or 3 in most cases) would lie between t_i and t_{i+1} (Fig. 10).

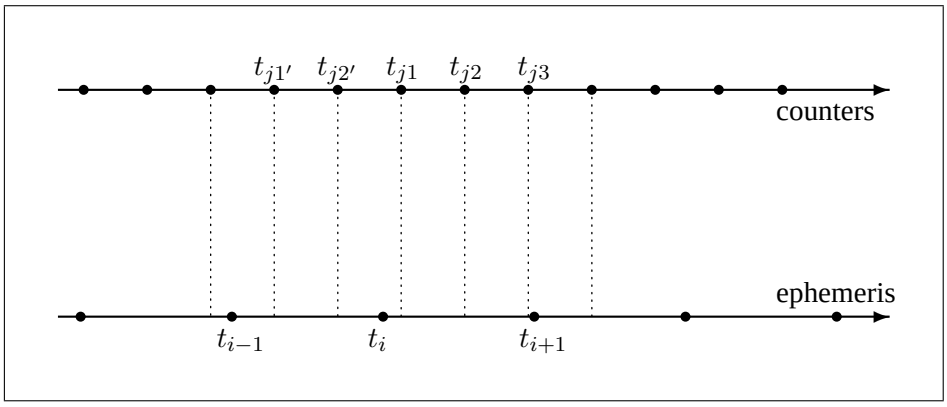

Figure 10: Different time scales for the ephemeris and counter data are re-adjusted.

For the MAPSview database, we deploy the read-out times of the counters, t_j, while the emphemeris data is kept constant using its last value between two subsequent t_j's. This means that no interpolation of t_i's is performed.

Bibliography

[1] Göller J.R. & Grün E. (1989): “Calibration of the Galileo/Ulysses dust detectors with different projectile materials and at varying impact angles”, *Planetary and Space Science 37*, Oct. 1989, p1197–1206.

[2] Grün E., Fechtig H., Hanner M.S, Kissel J., Lindblad B.-A., Linkert D., Maas D., Morfill G., Zook H.A. (1992): “The Galileo Dust Detector”, *Space Science Reviews 60*, p317–340.

[3] Kempf S. (2006a): “CDA Database” (cdaDB.pdf), Guide to the CDA database, available in an electronic version at the Max-Planck-Institute for Nuclear Physics, Heidelberg, or by the author.

[4] Kempf S. (2006b): “CDA Data Processing Tool” (cdaGUI.pdf), Manual for the GUI Data Viewer, available in an electronic version at the Max-Planck-Institute for Nuclear Physics, Heidelberg, or by the author.

[5] Kempf S. (2008): “Interpretation of high rate dust measurements with the Cassini dust detector CDA”, *Planetary and Space Science 56*, p378–385.

[6] Kempf S. (2012): “The Cosmic Dust Analyser Data Handbook” (cdaDataHB.pdf), available in an electronic version at `http://atmos.nmsu.edu/data_and_services/atmospheres_data/Cassini/cda.html` or by the author.

[7] Krüger H. (2003): “Jupiter’s Dust Disc: An Astrophysical Laboratory”, Shaker Verlag, Aachen. Habilitation Thesis at the Ruprecht-Karls-Universität, Heidelberg.

[8] Srama R. (2000): “Vom Cosmic-Dust-Analyser zur Modellbeschreibung wissenschaftlicher Raumsonden”, PhD thesis, Technische Universität München.

[9] Srama R. (2009): “Cassini-Huygens and Beyond — Tools for Dust Astronomy”, Habilitation treatise at the University of Stuttgart.

Acknowledgements

This work was kindfully supported by the Klaus Tschira Foundation, Heidelberg, at grant no. 00.161.2010.